

## OPEN

# 4-Methylumbelliferone Suppresses Hyaluronan Synthesis and Tumor Progression in SCID Mice Intra-abdominally Inoculated With Pancreatic Cancer Cells

Hayato Nagase, MD,\* Daisuke Kudo, MD, PhD,\* Akiko Suto, MD,\* Eri Yoshida, MD,\* Shinichiro Suto, PhD,† Mika Negishi, PhD,† Ikuko Kakizaki, PhD,† and Kenichi Hakamada, MD, PhD\*

**Objectives:** Pancreatic ductal adenocarcinoma contains large amounts of the glycosaminoglycan hyaluronan (HA), which is involved in various physiological processes. Here, we aimed to clarify the anticancer mechanisms of 4-methylumbelliferone (MU), a well-known HA synthesis inhibitor.

**Methods:** MIA PaCa-2 human pancreatic cancer cells were used. We evaluated cellular proliferation, migration, and invasion in the presence of MU, exogenous HA, and an anti-CD44 antibody. We also analyzed apoptosis, CD44 expression, and HA-binding ability using flow cytometry. The HA content in tumor tissue was quantified and histopathologically investigated in mice who had been inoculated with cancer cells.

**Results:** In vitro, MU inhibited pericellular HA matrix formation; however, *HAS3* mRNA was up-regulated. Treatment with 0.5 mM MU suppressed cellular proliferation by 26.4%, migration by 14.7%, and invasion by 22.7%. Moreover, MU also significantly increased apoptosis. CD44 expression and HA-binding ability were not altered by MU. In vivo, MU suppressed HA accumulation in pancreatic tumors and improved survival times in tumor-bearing mice.

**Conclusions:** 4-Methylumbelliferone indirectly caused apoptosis in pancreatic cancer cells by inhibiting HA production. 4-Methylumbelliferone may be a promising agent in the treatment of pancreatic cancer.

**Key Words:** 4-methylumbelliferone, CD44, extracellular matrix, hyaluronan, pancreatic cancer

(*Pancreas* 2017;46: 190–197)

Pancreatic ductal adenocarcinoma (PDAC) is the most malignant of all solid cancers because of difficulties with early diagnosis and the poor response to chemotherapy. The 5-year survival rate for patients with PDAC after potentially curative resection is only 5.5% to 7.2%,<sup>1–3</sup> and mortality rates have gradually increased in patients with PDAC, particularly in Japan.<sup>4</sup> Thus, there is an urgent need for novel, effective treatment strategies for PDAC.

Pancreatic ductal adenocarcinoma has an abundant volume of desmoplastic stroma. Several studies have reported that this stroma contains large amounts of hyaluronan (HA).<sup>5,6</sup> Hyaluronan is a nonsulfated linear glycosaminoglycan composed of repeated  $\beta$ -1,4-GlcUA- $\beta$ -1,3-GlcNAc disaccharide units.<sup>7</sup> Hyaluronan is a major component of the extracellular matrix, which plays an important role in various physiological processes. The 3 types of HA

synthases (HAS1, HAS2, and HAS3) produce HA molecules of various molecular sizes, and hyaluronidases (HYALs) catabolize HA.<sup>8,9</sup> Hyaluronan is found in almost all tissues and is increased in tissues that are undergoing cell proliferation, regeneration, and repair, such as embryonic, inflamed, and tumor stromal tissues.<sup>10,11</sup> Increased HA levels in malignant tumor cells have been reported in various cancers,<sup>12–14</sup> and several studies have shown that HA-rich stroma promotes proliferation, migration, invasion, metastasis, angiogenesis, and drug resistance in response to anticancer agents.<sup>15–17</sup> In addition, patients with HA-rich PDAC have been shown to have a lower survival rate.<sup>18</sup> CD44, a major HA receptor that is localized on the cell membrane, is a stem cell marker for PDAC.<sup>19</sup> Moreover, the interaction between HA and CD44 has been shown to promote tumor progression in several types of cancer.<sup>20</sup> Thus, HA and CD44 may provide novel therapeutic approaches for the control of the stromal environment in PDAC; this may be particularly true for HA.

In a previous study from our laboratory, we found that 4-methylumbelliferone (MU) inhibits HA synthesis and the formation of the pericellular matrix, which contains HA, in human skin fibroblasts.<sup>21</sup> Moreover, we have shown that the inhibition of HA synthesis is a result of depletion of uridine diphosphate glucuronic acid (UDP-GlcUA) and the down-regulation of HAS.<sup>22,23</sup> Thus, MU has been used as an HA synthesis inhibitor and proposed as a novel anticancer agent for various cancers.<sup>24–28</sup> We have also shown that MU exhibits anticancer properties in mouse melanoma cells and human pancreatic cancer cells.<sup>29–32</sup> Nakazawa et al<sup>32</sup> demonstrated that MU inhibits HA production and pericellular matrix formation in KPI-NL pancreatic cancer cells and decreases liver metastases in mice injected with pancreatic cancer cells.

However, the mechanisms through which HA production and subsequent anticancer activities are inhibited by MU are still unknown. Moreover, although CD44 is a marker of pancreatic cancer stem cells, no studies have reported whether MU alters the expression and activity of CD44 in pancreatic cancer cells. Therefore, in this study, we examined both the anticancer properties of MU in MIA PaCa-2 human pancreatic cancer cells and the influence of MU on CD44 expression and activity.

## MATERIALS AND METHODS

### Materials

4-Methylumbelliferone and *Streptomyces* HYAL were purchased from Wako Pure Chemicals (Osaka, Japan). High-molecular-weight HA (HMW-HA,  $1.2 \times 10^6$  d) was supplied by the Department of Glycotechnology, Hirosaki University. The Dulbecco modified Eagle medium was purchased from Nacalai Tesque Inc (Kyoto, Japan).

### Cell Culture

MIA PaCa-2 cells were a kind gift from the Department of Pharmacy, Hirosaki University Hospital (Hirosaki, Japan). The

From the Departments of \*Gastroenterological Surgery and †Glycotechnology, Hirosaki University Graduate School of Medicine, Hirosaki, Japan.

Received for publication November 21, 2015; accepted August 31, 2016.

Address correspondence to: Kenichi Hakamada, MD, PhD, Gastroenterological Surgery, Hirosaki University Graduate School of Medicine, 5 Zaifu-cho, Hirosaki, Aomori, Japan 036-8562 (e-mail: hakamada@hirosaki-u.ac.jp).

The authors declare no conflict of interest.

Copyright © 2016 The Author(s). Published by Wolters Kluwer Health, Inc. This is an open-access article distributed under the terms of the Creative Commons Attribution-Non Commercial-No Derivatives License 4.0 (CCBY-NC-ND), where it is permissible to download and share the work provided it is properly cited. The work cannot be changed in any way or used commercially without permission from the journal.

DOI: 10.1097/MPA.0000000000000741

cells were grown as monolayers at 37°C in an atmosphere containing 5% CO<sub>2</sub> with Dulbecco medium Eagle medium supplemented with 10% heat-inactivated fetal bovine serum, L-glutamine, sodium pyruvate, 100 µg/mL streptomycin, 100 IU/mL penicillin, and 0.25 µg/mL amphotericin B.

## Mice

CB17/Icr-SCID mice were purchased from Japan Clea (Tokyo, Japan). The mice were housed under specific pathogen-free conditions with a controlled light-dark cycle, temperature, and humidity; mice received water and food ad libitum and were used in the study after reaching 7 weeks of age and a weight of approximately 25 g. All animal experiments were performed according to the Guidelines for Animal Experimentation of Hiroasaki University.

## Particle Exclusion Assay

Pericellular matrices were visualized using a particle exclusion assay. Fixed horse erythrocytes (Nippon Biotest Laboratories Inc, Tokyo, Japan) were reconstituted in phosphate-buffered saline (PBS) at a density of  $5 \times 10^8$  cells/mL. The cells were cultured in 100-mm dishes. After 48 hours of incubation, we added serial concentrations of MU. The pericellular matrix was visualized by adding the horse erythrocyte suspension to the dishes and viewing them under a light microscope. To determine whether the pericellular matrix was composed of HA, the MU-free dishes were preincubated for 2 hours with 1.0 U/mL *Streptomyces* HYAL prior to the assay. Quantification of the cell surface halo was carried out using Image J software (US National Institutes of Health, Bethesda, Md).

## HA-Binding Assay and CD44 Expression by Fluorescence-Assisted Cell Sorting

The cells were incubated with serial concentrations of MU for 48 hours. Hyaluronan binding was detected by incubation with fluorescein-labeled HA (20 µg/100 µL; cat. no. 385906; EMD Biosciences, San Diego, Calif) for 30 minutes at 4°C. CD44 expression was detected by incubation with an Alexa Fluor 488-labeled anti-mouse/human CD44 antibody (cat. no. 103016; BioLegend, San Diego, Calif) or an isotype control (cat. no. 400625; BioLegend) for 30 minutes at 4°C. In both assays, the cells were harvested using Cell Dissociation Buffer (cat. no. S-014-C; EMD Millipore Corporation, Billerica, Mass) and a cell scraper in order to avoid cell-surface receptor cleavage. Hyaluronan binding and CD44 expression were analyzed using a flow cytometer (FACSARIA II; BD Biosciences, San Jose, Calif), and the data were analyzed using WinMDI software (The Scripps Research Institute, La Jolla, Calif).

## Quantitative Real-Time Polymerase Chain Reaction

Real-time polymerase chain reaction (RT-PCR) was carried out using an Omniscript RT kit (Qiagen, Tokyo, Japan). A MiniOpticon Real-Time PCR Detection System and a SYBR-Green Supermix (both from Bio-Rad Laboratories, Hercules, Calif) were used for the quantification of specific mRNAs. Amplification of *GAPDH* cDNA was performed to standardize the target cDNA levels. The primer sequences were as follows: *CD44*, AAGGCTGGGGCTCATTGCGAG/CCAAATTCGTTGTCATAC CAGG; *HAS1*, TGCTCAGCATGGGTTATGC/AGGGCGTCTCT GAGTAGCAG; *HAS2*, CTCGGGACCACACAGAC/TCAGGAT ACATAGAAACCTCTCAC; *HAS3*, ACCATCGAGATGCTT CGAGT/CCATGAGTCTGACTTGTGAGG; and *GAPDH*, AGCC ACATCGCTCAGACAC/GCCCAATACGACCAATCC. The expression levels of the specific genes were shown as fold changes compared with the controls.

## Proliferation Assay

The cells ( $1 \times 10^5$  cells/well) were seeded into 6-well plates. After 24 hours of incubation, we added serial concentrations of MU, an anti-CD44 monoclonal antibody (KM81; 10 µg/mL; ab112178; Abcam, Tokyo, Japan), and/or HMW-HA (0.5 mg/mL). After incubation periods of 24, 48, or 72 hours, the adhered cells were removed using trypsin, resuspended with PBS, and assessed using an automated cell counter (TC20; Bio-Rad, Tokyo, Japan).

## Wound Healing Assay

The cells ( $1 \times 10^5$  cells/well) were cultured in 24-well plates and incubated. After confirming the formation of a complete monolayer, the cells were wounded by scratching with a standard 200-µL plastic tip, and serial concentrations of MU, KM81 (10 µg/mL), and/or HMW-HA (0.5 mg/mL) were added. Migration and cell movement throughout the wound area were observed with a phase-contrast microscope after 48 hours. The percentage of filled wound area was calculated as follows: filled wound area (%) = (original wound area – remaining wound area) / original wound area  $\times$  100.

## Invasion Assay

Invasion assays were performed using Matrigel Invasion Chambers (BD Bioscience, Franklin Lakes, NJ). Cells that had been preincubated with serial concentrations of MU for 48 hours were resuspended at  $1 \times 10^6$  cells/mL in serum-free culture medium, and 500 µL of the cell suspension was placed in the upper chamber. Dulbecco medium Eagle medium containing 10% fetal bovine serum with or without HA (0.5 mg/mL) was added to the lower chamber. After incubation for 22 hours at 37°C in an atmosphere containing 5% CO<sub>2</sub>, the filters were stained with hematoxylin. The cells that migrated through the membrane were counted as follows: relative invasion = (number of cells migrating under experimental conditions) / (number of cells migrating under control conditions)  $\times$  100%.

## Apoptosis Assay

Apoptosis assays were carried out using annexin V and propidium iodide (PI) by flow cytometry. Tumor cells were cultured in the presence or absence of serial concentrations of MU for 48 hours. Next, the cells were stained with annexin V and PI for 15 minutes at room temperature. A FACSARIA II flow cytometer was used to acquire data for analysis using WinMDI (The Scripps Research Institute, La Jolla, Calif).

## Tumor Inoculation

In our preliminary experiment, inoculation with MIA PaCa-2 cells resulted in tumor formation in the pancreas of SCID mice at 5 weeks after intra-abdominal cancer cell implantation. A suspension of tumor cells ( $2.0 \times 10^6$  cells/0.2 mL PBS) was injected into the abdomens of the mice. Tumor-bearing mice were randomly divided into 2 groups that were treated with or without MU. After 1 week, the mice received MU orally at a dose of 2 mg/g body weight every day. The conditions of these mice were checked each day. The survival time was compared between the 2 groups of SCID mice by log-rank analysis of Kaplan-Meier curves.

## Analysis of HA Synthesis in Pancreatic Cancer

The dry weight of each tumor sample was measured after desiccation at 60°C for 4 hours. Each sample was treated with 1 mL of 0.25% actinase E/10 mM Tris-HCl (pH 8.0) and incubated for 24 hours at 55°C, followed by incubation at 100°C for 10 minutes to stop the reaction. After centrifugation, the supernatant was removed, and the HA levels in the solution were measured using a

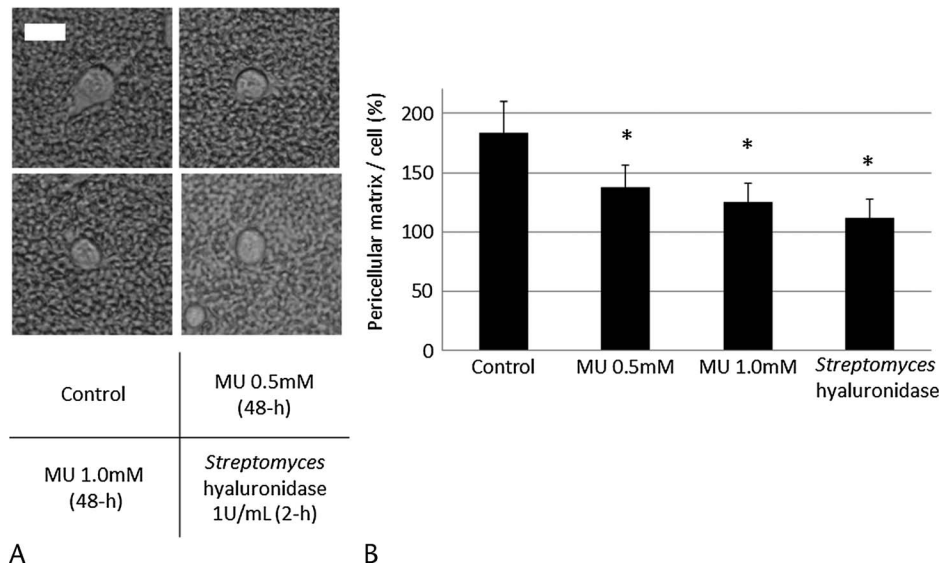


**FIGURE 1.** Effects of MU on the pericellular matrix in MIA PaCa-2. A, The pericellular matrix was visualized using a particle exclusion assay. The scale bar is 20  $\mu$ m. B, The pericellular matrix area/cell area was analyzed using Image J software. Each data point is the mean  $\pm$  SD of 3 experiments (20 cells analyzed per experiment). \* $P < 0.05$ .

sandwich binding protein assay kit in accordance with the manufacturer's protocol (Biotech Trading Partners, Encinitas, Calif).

### HA Staining of Tumor Tissues

The mice were killed 5 weeks after intra-abdominal implantation of the tumor cells. The tumors were removed, fixed in 10% formalin, and placed in 70% ethanol and 5% glacial acetic acid. The samples were embedded in paraffin using routine procedures, sliced at a thickness of 4  $\mu$ m, and analyzed using an iVIEW DAB Detection Kit (Ventana Medical Systems, Tucson, Ariz). Antigen retrieval was performed using Cell Conditioning Solution (CCI-Tris-based EDTA buffer; pH 8.0; Ventana Medical Systems), and the tissue samples were incubated for 32 minutes at 37°C with 2.5  $\mu$ g/mL biotinylated HA-binding protein.

### Statistical Analysis

Statistical comparisons were carried out using 2-tailed Student's *t*-test, and differences with  $P < 0.05$  were accepted as statistically significant.

## RESULTS

### MU Decreased the Pericellular Matrix Containing HA in MIA PaCa-2 Cells

The size of the pericellular matrix was measured using a particle exclusion assay. We found that MU- and *Streptomyces* HYAL-pretreated MIA PaCa-2 cells had less pericellular matrix than cells preincubated without MU (Fig. 1A). The ratio of the pericellular matrix area to the cell area is shown in Figure 1B. 4-Methylumbelliferone and *Streptomyces* HYAL significantly decreased the amount of HA-containing pericellular matrix.

### MU Did Not Alter the Expression of CD44 or the Ability to Bind HA in MIA PaCa-2 Cells

The results of the CD44 expression and HA-binding assay by fluorescence-assisted cell sorting are shown in Figure 2. Almost all MIA PaCa-2 cells (99.0%) have been reported to express CD44, the main cell-surface receptor for HA.<sup>33</sup> Similarly, in our

assay, almost all MIA PaCa-2 cells (99.9%) expressed CD44 and had the ability to bind to exogenous HA. The results of the HA-binding assay and the CD44 expression analysis by fluorescence-assisted cell sorting were not affected by pretreatment with MU at 1.0 mM (Figs. 2A, B). In addition, using real-time RT-PCR, we found that the level of *CD44* mRNA expression was not changed by pretreatment with MU at 1.0 mM (Fig. 2C).

### MU Altered HAS3 mRNA Expression in MIA PaCa-2 Cells

*HAS* mRNA expression was measured using real-time RT-PCR. Of the 3 types of HASs, only HAS3 levels could be measured. Real-time RT-PCR revealed that treatment with MU at 1.0 mM for 48 hours up-regulated the expression of *HAS3* mRNA by 1.67 fold ( $P < 0.05$ ; Fig. 2C).

### MU Inhibited Cell Proliferation, Migration, and Invasion in MIA PaCa-2 Cells

Next, we examined the effects of MU on cell proliferation, migration, and invasion in MIA PaCa-2 cells. We used anti-CD44 monoclonal antibodies in proliferation and wound-healing assays to assess the function of HA-CD44 interactions. In addition, we examined whether exogenous HMW-HA abrogated the changes induced by MU. The effects of MU on cell proliferation are shown in Figure 3A. After 72 hours of treatment, MU inhibited cell proliferation in a concentration-dependent manner. Cancer cells treated with MU (0.5 mM) and KM81 (10  $\mu$ g/mL) were significantly inhibited by 26.4% and 29.7%, respectively ( $P < 0.05$ ). The addition of exogenous HMW-HA did not alter cell proliferation. 4-Methylumbelliferone also suppressed the amount of cell migration and invasion, as determined by wound-healing assays and the Matrigel invasion assay, by 14.7% and 22.7%, respectively ( $P < 0.05$ ; Figs. 3B, C). In addition, blocking CD44 significantly inhibited cell migration by 16.2% ( $P < 0.05$ ). The addition of HMW-HA (0.5 mg/mL) increased the amount of cell migration and invasion to the levels of the control group.



## MU Induced Apoptosis in MIA PaCa-2 Cells

The levels of apoptosis were determined by annexin V/PI staining (Fig. 4). The results showed that treatment with MU for 48 hours led to a concentration-dependent increase in apoptosis in MIA PaCa-2 cells. The difference between the values for the control cells and the MU-treated (0.1 mM) cells did not reach statistical significance (data not shown). The percentage of apoptotic cells was significantly increased in cells treated with MU (0.5 mM;  $P < 0.05$ ).

## MU Inhibited HA Production and Improved Survival Times in Mice

Tumor formation was found in the pancreas of all mice used in our study, and almost all the mice died of severe carcinomatous peritonitis. We analyzed the differences in survival times between untreated and MU-treated mice using log-rank analysis of Kaplan-Meier curves. The survival time of MU-treated mice (43.6 days) was significantly longer than that in untreated mice (40.8 days;  $P < 0.05$ , Fig. 5A). 4-Methylumbelliferone did not have an inhibitory effect on tumor weight (data not shown), but inhibited HA production in pancreatic tumors. Analysis of HA staining revealed that HA retention in MU-treated tumors was significantly lower than that in control tumors (Fig. 5B). In addition, we evaluated the amount of HA in pancreatic tumors and found that MU significantly inhibited HA production in pancreatic tumors (Fig. 5C).

## DISCUSSION

Most cancers are rich in HA,<sup>5,12–14</sup> and HA-rich stroma promotes tumorigenic activity.<sup>15–17</sup> Interactions between HA and its cell membrane receptors, such as CD44 and RHAMM, regulate tumor development and progression.<sup>20</sup> In addition, the pericellular

HA matrix of cancer cells acts as a barrier against the immunocompetent cells of the host.<sup>34</sup> Therefore, targeting HA by MU may be a novel therapeutic approach for controlling HA levels in the cancer cell stroma. We have previously revealed that MU exhibits anticancer activity in C57BL6 mice inoculated with melanoma cells<sup>29</sup>; we subsequently revealed the efficacy of MU in human pancreatic cancer cells in both in vitro and in vivo.<sup>32</sup> 4-Methylumbelliferone was then later shown to inhibit HA production and to have anticancer activities in mouse models of various cancers.<sup>24,25,27,28</sup> Moreover, HA has recently been shown to promote cancer progression.<sup>9,16</sup> In this study, exogenous HMW-HA did not influence the proliferation of MIA PaCa-2 cells but did abrogate the effects of MU on migration and invasion. There are several potential explanations for these findings. First, exogenous and pericellular HAs exhibit different biological functions. In addition, exogenous HMW-HA promotes migration and invasion in MIA PaCa-2 cells, as described in a previous report.<sup>35</sup> Third, the molecular length of HA (HMW,  $1.2 \times 10^6$  d) may not be suitable for treatment of MIA PaCa-2 cells. In our study, only *HAS3* mRNA could be detected in MIA PaCa-2 cells, and researchers have reported that *HAS3* produces lower-molecular-weight HA than other *HASs*, such as *HAS1* and *HAS2*.<sup>8</sup> In addition, HA has been shown to have distinctly different biological functions depending on the length of the chain.<sup>9</sup> The 1.67-fold increase in *HAS3* mRNA expression may have resulted from compensation for HA deficiency in a suitable microenvironment for cancer progression. Nonetheless, HA synthesis was suppressed by MU, and cellular proliferation, migration, and invasion were also reduced.

Studies have shown that MU inhibits HA synthesis in at least 2 ways. First, MU depletes UDP-GlcUA, which is a precursor of HA.<sup>22</sup> Second, MU reduces the expression of *HAS* mRNA.<sup>23</sup> However, no studies have described the mechanisms through which

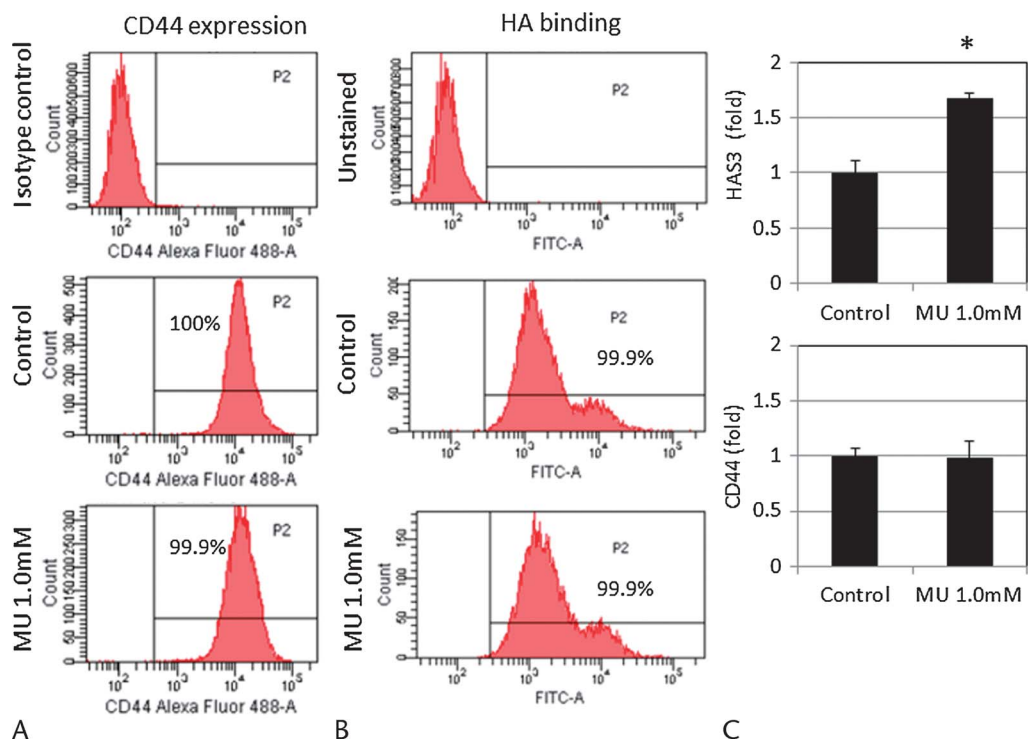


**FIGURE 2.** Effects of MU on CD44 and HAS expression in MIA PaCa-2. A, Expression of CD44 and (B) HA binding in MIA PaCa-2 cells after treatment with or without MU (1.0 mM). The isotype control and cells without HA–fluorescein isothiocyanate staining are each shown in the figure. These results are representative of 3 independent experiments. C, *HAS3* and *CD44* mRNA levels were measured in MIA PaCa-2 cells by real-time RT-PCR. Each bar represents the mean  $\pm$  SD of 3 replications. \* $P < 0.05$ .

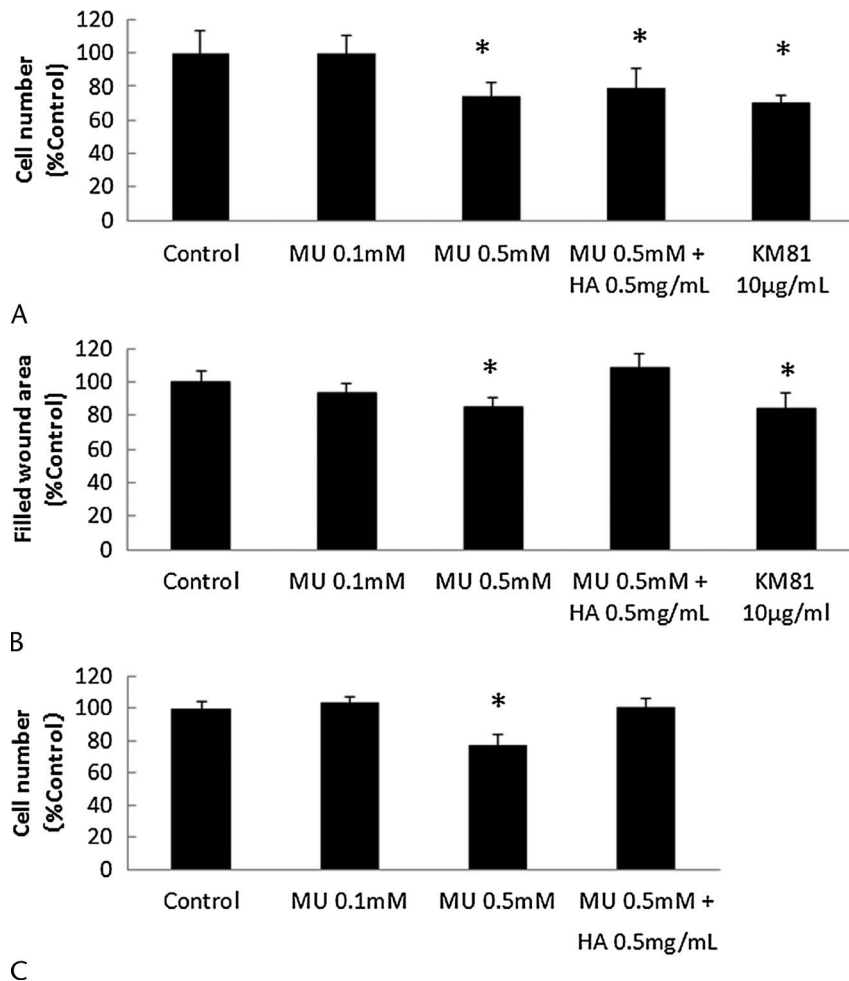


**FIGURE 3.** Proliferation, migration, and invasion of MIA PaCa-2 cells. The effects of MU on cell proliferation (A), migration (B), and invasion (C) were evaluated in MIA PaCa-2 cells. Each bar represents the mean  $\pm$  SD of 3 replications. \* $P < 0.05$ .

MU reduces *HAS* mRNA expression. Some reports have indicated that *HAS* mRNA expression is suppressed by MU,<sup>23,24,27</sup> whereas another report indicated that *HAS* mRNA expression is up-regulated.<sup>25</sup> The results of our study supported the latter findings. We hypothesized that the up-regulation of the *HAS3* mRNA expression resulted from positive feedback from the decreased HA production in MIA PaCa-2 cells. Notably, whether HA reduction by MU causes positive or negative feedback may depend on the type of cancer cells, suggesting that the inhibition of HA synthesis in MIA PaCa-2 cells may be caused by depletion of UDP-GlcUA and not by down-regulation of *HAS* mRNA.

Some studies have indicated that MU decreases CD44 expression in human prostate and breast cancer cells<sup>24,36</sup>; however, other studies have shown that MU does not alter CD44 expression in human osteosarcoma and breast cancer cells.<sup>23,25</sup> In our study, MU did not have a direct effect on CD44 expression, and the ability to bind exogenous HA was not altered by MU in MIA PaCa-2 cells. These findings suggested that HA depletion by MU inhibited the HA-CD44 interaction, which consequently resulted in anticancer effects. CD44 has recently been identified as a marker of pancreatic cancer stem cells, along with ESA and CD24.<sup>19</sup> Thus, these proteins may represent novel therapeutic targets because they are associated with recurrence, metastasis, and drug resistance in cancers.<sup>20</sup> Blocking the HA-CD44 interaction with a monoclonal antibody resulted in the suppression of cell proliferation and

migration in our study. Anti-CD44 antibodies may be effective in pancreatic cancer therapy; however, such an approach would be expensive and require a long process for clinical application and approval in patients with pancreatic cancer. In contrast, MU, an inexpensive compound, is more likely to be used clinically in the future because it is widely available as an oral choleric agent. Thus, MU therapy may become a targeted therapy for pancreatic cancer stem cells because of inhibition of the HA-CD44 interaction.

We have previously reported that MU inhibits HA synthesis in tumor in SCID mice after subcutaneous implantation with pancreatic cancer cells.<sup>37</sup> We have also shown that MU suppresses liver metastasis in SCID mice implanted with pancreatic cancer cells into their spleens.<sup>32</sup> In this study, pancreatic cancer cells were intra-abdominally injected, and our results indicated that orally administered MU could be distributed throughout the entire body and could exert anticancer activity toward pancreatic cancer cells. This systemic distribution of MU may be suitable for the treatment of PDAC because lymph node and distant metastases frequently occur in patients with PDAC. However, the MU-dependent inhibition of HA synthesis and anticancer activity were insufficient compared with that described in other reports.<sup>25,28,38</sup> These results could be explained as follows. First, the pancreatic tumors in mice were extremely desmoplastic and had abundant HA. Second, CD44 was expressed at high levels in MIA PaCa-2 cells. As a result, the indirect anticancer activity of MU, which was induced via

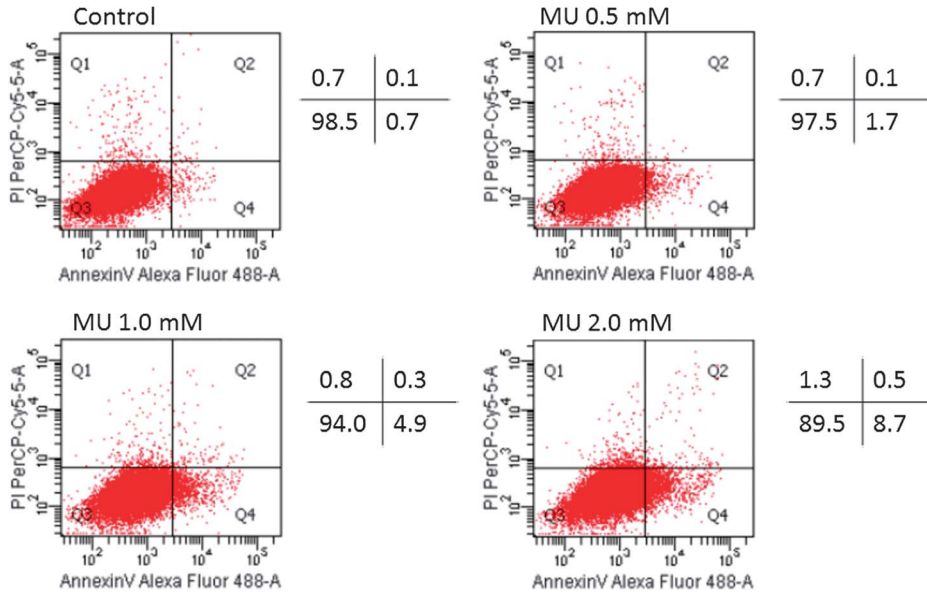


**FIGURE 4.** Induction of apoptosis by MU in MIA PaCa-2 cells. Apoptosis in MIA PaCa-2 cells was evaluated using annexin V/PI. The proportions of apoptotic cells and living cells are shown. These results are representative of 3 independent experiments.

inhibition of HA production, was insufficient. To resolve this problem, combination therapy of MU plus other cytotoxic anticancer agents may improve outcomes. We have previously reported that gemcitabine plus MU therapy is more effective than gemcitabine alone in vivo.<sup>32</sup> We also showed that MU increases the intracellular concentration of 5-fluorouracil by decreasing the pericellular

HA barrier and that 5-fluorouracil plus MU therapy is effective in vivo (data not shown). Thus, future studies are needed to further assess the efficacy and complications of combination therapies including MU.

4-Methylumbelliferone has been widely used as a choleric agent. Clinical trials in humans have shown that MU has minimal

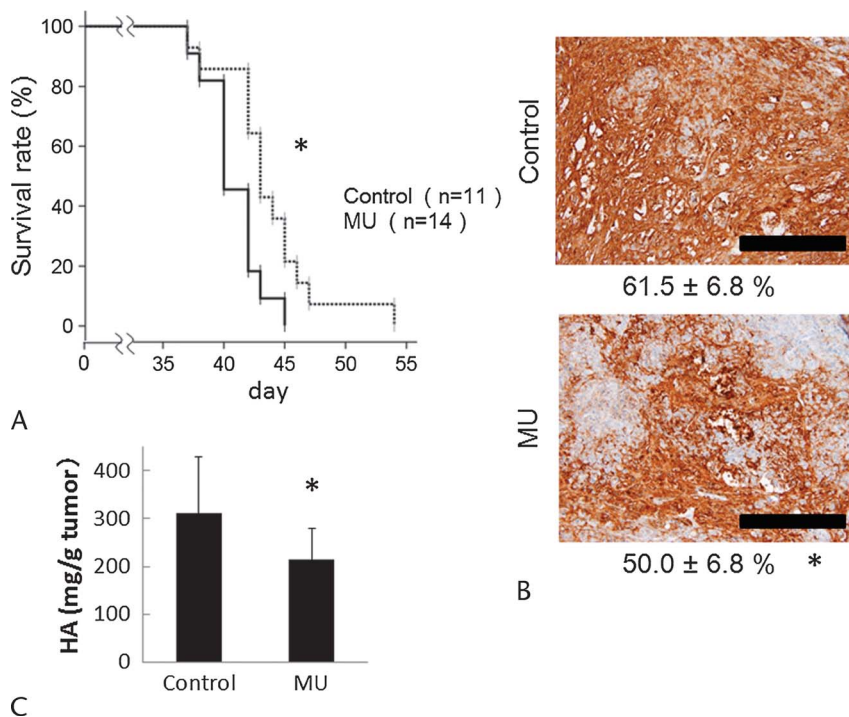


**FIGURE 5.** Anticancer effects of MU in vivo. **A**, Survival of mice was evaluated by Kaplan-Meier curve. \* $P < 0.05$  versus the control group using log-rank tests. **B**, The HA-positive area of pancreatic tumors was determined using immunohistochemical staining with HA-binding protein. The numbers below each panel are the mean HA-positive area  $\pm$  SD (\* $P < 0.05$ ). Black bars represent 100  $\mu$ m. **C**, Hyaluronan quantification was analyzed as described in Materials and Methods. Each bar represents the mean value  $\pm$  SD (\* $P < 0.05$ ).

adverse effects when used at the approved oral dose of 900 to 2400 mg/d in adults.<sup>39</sup> However, the safety of oral MU doses greater than 2400 mg/d and for treatment periods of more than 3 months has not been established. Moreover, no trials have been performed in patients with cancer. Therefore, it will be necessary to determine the appropriate oral dose of MU for achieving its anticancer effects and to assess complications during clinical trials.

In conclusion, our findings showed that MU had anticancer properties in a pancreatic cancer cell line and improved survival times in mice with pancreatic tumors. The results of our study suggested that MU may have effectiveness as a novel anticancer agent for the treatment of pancreatic cancer.

### ACKNOWLEDGMENTS

The authors thank Prof Hiroshi Kijima and Dr Satoko Morohashi, Department of Pathology and Bioscience, Hirosaki University, Graduate School of Medicine, for excellent technical assistance. They also thank Dr Toshiyuki Yamada, Biochemistry and Genome Biology, Hirosaki University Graduate School of Medicine, for technical advice on the experiments.

### REFERENCES

- Matsuda T, Ajiki W, Marugame T, et al. Population-based survival of cancer patients diagnosed between 1993 and 1999 in Japan: a chronological and international comparative study. *Jpn J Clin Oncol*. 2011;41:40–51.
- Sant M, Allemani C, Santaquilani M, et al. EURO-CARE-4. Survival of cancer patients diagnosed in 1995–1999. Results and commentary. *Eur J Cancer*. 2009;45:931–991.
- Howlander N, Noone AM, Krapcho M, et al. (eds). SEER Cancer Statistics Review, 1975–2012, National Cancer Institute. Bethesda, MD. November 18, 2015. Available at: [http://seer.cancer.gov/csr/1975\\_2012/](http://seer.cancer.gov/csr/1975_2012/). Accessed April 5, 2016.
- Imamura Y, Mizuno S. Comparison of pancreatic cancer mortality in five countries: France, Italy, Japan, UK and USA from WHO mortality database (1960–2000). *Jpn J Clin Oncol*. 2005;35:283–286.
- Theocharis AD, Tsara ME, Papageorgacopoulou N, et al. Pancreatic carcinoma is characterized by elevated content of hyaluronan and chondroitin sulfate with altered disaccharide composition. *Biochim Biophys Acta*. 2000;1502:201–206.
- Fries H, Elsässer HP, Mahlbacher V, et al. Localisation of hyaluronate (HA) in primary tumors and nude mouse xenografts of human pancreatic carcinomas using a biotinylated HA-binding protein. *Virchows Arch*. 1994;424:7–12.
- Weissmann B, Rapport MM, Linker A, et al. Isolation of the aldobionic acid of umbilical cord hyaluronic acid. *J Biol Chem*. 1953;205:205–211.
- Itano N, Sawai T, Yoshida M, et al. Three isoforms of mammalian hyaluronan synthases have distinct enzymatic properties. *J Biol Chem*. 1999;274:25085–25092.
- Karbownik MS, Nowak JZ. Hyaluronan: towards novel anti-cancer therapeutics. *Pharmacol Rep*. 2013;65:1056–1074.
- Toole BP. Hyaluronan promotes the malignant phenotype. *Glycobiology*. 2002;12:37R–42R.
- Alaniz L, Garcia M, Rizzo M, et al. Altered hyaluronan biosynthesis and cancer progression: an immunological perspective. *Mini Rev Med Chem*. 2009;9:1538–1546.
- Ropponen K, Tammi M, Parkkinen J, et al. Tumor cell-associated hyaluronan as an unfavorable prognostic factor in colorectal cancer. *Cancer Res*. 1998;58:342–347.
- Setälä LP, Tammi MI, Tammi RH, et al. Hyaluronan expression in gastric cancer cells is associated with local and nodal spread and reduced survival rate. *Br J Cancer*. 1999;79:1133–1138.
- Lipponen P, Aaltomaa S, Tammi R, et al. High stromal hyaluronan level is associated with poor differentiation and metastasis in prostate cancer. *Eur J Cancer*. 2001;37:849–856.
- Itano N, Zhuo L, Kimata K. Impact of the hyaluronan-rich tumor microenvironment on cancer initiation and progression. *Cancer Sci*. 2008;99:1720–1725.
- Sironen RK, Tammi M, Tammi R, et al. Hyaluronan in human malignancies. *Exp Cell Res*. 2011;317:383–391.
- Toole BP. Hyaluronan-CD44 interactions in cancer: paradoxes and possibilities. *Clin Cancer Res*. 2009;15:7462–7468.
- Cheng XB, Sato N, Kohi S, et al. Prognostic impact of hyaluronan and its regulators in pancreatic ductal adenocarcinoma. *PLoS One*. 2013;8:e80765.
- Li C, Heidt DG, Dalerba P, et al. Identification of pancreatic cancer stem cells. *Cancer Res*. 2007;67:1030–1037.
- Misra S, Hascall VC, Markwald RR, et al. Interactions between hyaluronan and its receptors (CD44, RHAMM) regulate the activities of inflammation and cancer. *Front Immunol*. 2015;6:201.
- Nakamura T, Takagaki K, Shibata S, et al. Hyaluronic acid-deficient extracellular matrix induced by addition of 4-methylumbelliferone to the medium of cultured human skin fibroblasts. *Biochem Biophys Res Commun*. 1995;208:470–475.
- Kakizaki I, Kojima K, Takagaki K, et al. A novel mechanism for the inhibition of hyaluronan biosynthesis by 4-methylumbelliferone. *J Biol Chem*. 2004;279:33281–33289.
- Kulti A, Pasonen-Seppänen S, Jauhiainen M, et al. 4-Methylumbelliferone inhibits hyaluronan synthesis by depletion of cellular UDP-glucuronic acid and downregulation of hyaluronan synthase 2 and 3. *Exp Cell Res*. 2009;315:1914–1923.
- Lokeshwar VB, Lopez LE, Munoz D, et al. Antitumor activity of hyaluronic acid synthesis inhibitor 4-methylumbelliferone in prostate cancer cells. *Cancer Res*. 2010;70:2613–2623.
- Arai E, Nishida Y, Wasa J, et al. Inhibition of hyaluronan retention by 4-methylumbelliferone suppresses osteosarcoma cells in vitro and lung metastasis in vivo. *Br J Cancer*. 2011;105:1839–1849.
- Lompardía SL, Papademetrio DL, Mascaró M, et al. Human leukemic cell lines synthesize hyaluronan to avoid senescence and resist chemotherapy. *Glycobiology*. 2013;23:1463–1476.
- Urakawa H, Nishida Y, Wasa J, et al. Inhibition of hyaluronan synthesis in breast cancer cells by 4-methylumbelliferone suppresses tumorigenicity in vitro and metastatic lesions of bone in vivo. *Int J Cancer*. 2012;130:454–466.
- Piccioni F, Malvicini M, Garcia MG, et al. Antitumor effects of hyaluronic acid inhibitor 4-methylumbelliferone in an orthotopic hepatocellular carcinoma model in mice. *Glycobiology*. 2012;22:400–410.
- Kudo D, Kon A, Yoshihara S, et al. Effect of a hyaluronan synthase suppressor, 4-methylumbelliferone, on B16F-10 melanoma cell adhesion and locomotion. *Biochem Biophys Res Commun*. 2004;321:783–787.
- Yoshihara S, Kon A, Kudo D, et al. A hyaluronan synthase suppressor, 4-methylumbelliferone, inhibits liver metastasis of melanoma cells. *FEBS Lett*. 2005;579:2722–2726.
- Morohashi H, Kon A, Nakai M, et al. Study of hyaluronan synthase inhibitor, 4-methylumbelliferone derivatives on human pancreatic cancer cell (KPI-NL). *Biochem Biophys Res Commun*. 2006;345:1454–1459.
- Nakazawa H, Yoshihara S, Kudo D, et al. 4-Methylumbelliferone, a hyaluronan synthase suppressor, enhances the anticancer activity of gemcitabine in human pancreatic cancer cells. *Cancer Chemother Pharmacol*. 2006;57:165–170.
- Wei HJ, Yin T, Zhu Z, et al. Expression of CD44, CD24 and ESA in pancreatic adenocarcinoma cell lines varies with local microenvironment. *Hepatobiliary Pancreat Dis Int*. 2011;10:428–434.

34. McBride WH, Bard JB. Hyaluronidase-sensitive halos around adherent cells. Their role in blocking lymphocyte-mediated cytotoxicity. *J Exp Med.* 1979;149:507–515.
35. Gouëffic Y, Guilluy C, Guérin P, et al. Hyaluronan induces vascular smooth muscle cell migration through RHAMM-mediated PI3K-dependent Rac activation. *Cardiovasc Res.* 2006;72:339–348.
36. Hiraga T, Ito S, Nakamura H. Cancer stem-like cell marker CD44 promotes bone metastases by enhancing tumorigenicity, cell motility, and hyaluronan production. *Cancer Res.* 2013;73:4112–4122.
37. Yoshida E, Kudo D, Nagase H, et al. Antitumor effects of the hyaluronan inhibitor, 4-methylumbelliferone, on pancreatic cancer. *Oncol Lett.* 2016; 12:2337–2344.
38. Piccioni F, Fiore E, Bayo J, et al. 4-Methylumbelliferone inhibits hepatocellular carcinoma growth by decreasing IL-6 production and angiogenesis. *Glycobiology.* 2015;25:825–835.
39. Nagy N, Kuipers HF, Frymoyer AR, et al. 4-Methylumbelliferone treatment and hyaluronan inhibition as a therapeutic strategy in inflammation, autoimmunity, and cancer. *Front Immunol.* 2015;6:123.